Assembly of Complex Shaped Objects : A Stiffness Control with Contact Localization

Sungchul Kang* Munsang Kim* and Kyo-Il Lee**

(*Received July 21, 1997*)

This paper presents a compliant control method for insertion of complex objects with concavities. The control algorithm presented here is capable of generating satisfactory compliant motion control in spite of changing contact states. During the execution of a nominal motion plan, it computes the actual position of the contact point from the force/torque sensor reading using a contact localization algorithm. It then dynamically updates the center of compliance to the computed contact point, and minimizes the chance of jamming and unwanted collisions. The control scheme has been implemented on hardware and tested on the task of inserting a T-shaped object into a C-shaped cavity with a very tight tolerance. The insertion motion, which involves a sequence of 2 translational and 1 rotational compliant motions, was successfully executed by the proposed compliant motion controller.

Key Words: Compliant Motion, Motion Planning, Insertion, Concave Object, Contact, Planar Robot, Contact Localization, Stiffness Control, Moving Compliance Frame, Real-Time Controller

1. Introduction

Most research efforts on robot assembly using compliant motion control schemes (Paul and Shimano, 1976; Salisbury, 1980) have focused on assembling objects having a simple geometry, e. g., peg-in-hole or electronic components and on overcoming jamming due to robot positioning errors or uncertain environments by correcting an insertion path using contact force/torque information (Whitney, 1977; Lee and Asada, 1994). Recently, various robot applications, such as assembly by mobile robots, teleoperation and robotic surgery, require an insertion of a complicated object into an uncertain environment. In these applications, the size of the entry hole is often smaller than some dimension of the peg, and multi-step compliant motions are required for insertion rather than a single motion. Even though there might be a non-contact insertion path, a contact path is often easier to execute. To meet these needs, an insertion technique which plans a contact path and executes a compliant motion needs to be developed to complement human skills and increase the autonomy of robotic systems.

This paper presents a control algorithm for insertion operations involving complex objects and multi-step compliant motions. The compliant motion control of a complex object is difficult for two reasons. First, there are many

more contact states than a simple peg-in-hole, and results in frequent contact state changes. Second, the magnitude of the changes, e. g., the distance between the new and previous contact points can be quite large, requiring the controller to reset the center of compliance. The key feature of the proposed compliant motion controller is 1) dynamic on-line sensing and computation of the contact point based on the readings from the wrist force/torque sensor, and 2) subsequent updating

*Advanced Robotics Research Center, KIST, Hawolgok-dong, Sungbuk-gu, Seoul, 136-791, Korea

**Department of Mechanical Design & Production Engineering, Seoul National University, Shinlim-dong, Kwanak-gu, Seoul, 151-742, Korea

of the center of compliance to minimize jamming and undesired collisions. Another contribution is the extension of the contact localization algorithm to rectangular objects.

Numerous results are available on both planning and control of motions under uncertainties. Planning is concerned with computing a nominal compliant motion from the robot controller model, object models and their associated uncertainties, while control algorithms are aimed at executing the planned motion in spite of uncertainties such as friction, control and sensing errors.

Compliant motion control can be achieved by either controlling the joint torques or by controlling the position command to a position-controlled manipulator. In the first approach, such as in stiffness control (Salisbury, 1980) or impedance control (Hogan, 1985), the desired stiffness or impedance can be obtained by controlling the joint torques during execution of a constrained motion. The controller is responsible for computing required joint torques to achieve a desired behavior. In the second approach (Paul and Shimano, 1976; Salisbury, 1980), robot compliance is achieved by controlling the command trajectory. An external positional feedback loop is typically required. There is somewhat different type of control scheme called the hybrid position/force control (Goldenberg and Song, 1996; Yong, 1997). It is motivated by the natural and the artificial constraints, and is aimed at tracking both the desired position and the force trajectory using the orthogonality (or reciprocity) between the position direction and the force direction to be controlled. Since compliant motions in assembly are usually required to be slow to avoid impact and need not follow force trajectories exactly, it is appropriate to adopt stiffness control which assumes a quasi-static motion rather than impedance control or hybrid position/force control.

There is an extensive work on contact analysis of the peg-in-a-hole problem. Vukobratovic and Stokic (1982) enumerated all possible contact states for this problem, and presented the conditions for jamming explicitly. Asada and Hirai (1989) developed a method to compute feasible motions for multiple-contact cases, and applied it to the peg-in-hole problem using polyhedral convex cones. It is used in assembly planning for computing feasible differential motion directions. As far as planning an insertion motion, Strip (1988) has proposed an oriented insertion technique by doing a contact analysis of various convex and star-shaped pegs using friction cones. More recently, Astuti and McCarragher (1996) and McCarragher (1996) has presented a discrete event controller imitating human decision making mechanism for dual-peg and two-tired peg insertion tasks. The transition among different contact states are modeled as a Markov process and a probabilistic controller has been developed.

Most existing results including the ones mentioned above are limited to insertion tasks involving prismatic objects moving along a 1-dimensional insertion path normal to the mating face. These tasks have the property that the cross section of the object being inserted is a subset of that of the hole or slot. In contrast, our insertion task involves a concave polyhedral peg and hole, and the number of contact states is dramatically increased (approximately quadratic in the number of convex subparts), posing a difficulty for the existing algorithms.

Localization methods of the contact point using force/torque information during insertion have been presented by Zhou, Shi and Li (1996) and Tsujimure and Yabuta (1988). The coordinates of the contact point are computed by intersecting object surface with the line representing the relationship between the sensed force and torque. When the contact point can be localized on-line, the compliance frame (or the center of compliance) and other control gain parameters can be adjusted dynamically during insertion to improve the controller performance. For example, a stiffness gain can be updated by considering the moving direction and the constraint direction with respect to the compliance frame corresponding to the contact point. In fact, this is one of the key features of our algorithm.

A seminal work on compliant motion planning is presented by Lozano-Perez, Mason and Taylor

(1984), where the concept of uncertainty cones is introduced and used to develop a planning methodology called *backprojection.* In this paradigm, motion is planned backward from the goal region toward the start point. For a given goal region, the uncertainty cone is used to compute a *preimage* such that if the robot starts in the preimage, it is guaranteed to reach the goal region. This computation is recursively done until the start point is included in one of the pre-images. The notions of goal recognizability and termination conditions are also important in compliant motion planning since the robot joint encoder readings alone cannot tell whether the goal is reached and when to stop motion commands. A number of results (Latombe, Lazanas and Shekhar, 1991) have followed, and the current status can be summarized as 1) the complexity of motion planning under uncertainty is exponential to the number of backprojection steps (Canny, 1989), 2) the backprojection regions are not unique and dependent on the termination condition (Erdmann, 1986), and 3) implementation is very difficult beyond 4 dimensions (Brost and Christiansen, 1994).

This paper is organized as follows. A complex insertion task is introduced and used to illustrate our algorithm in Sec. 2. The compliant motion control algorithm and hardware experimental results are presented in Sections 3 and 4, respectively. Finally, conclusions and future work are discussed in Sec. 5.

2. Task Analysis

For the remainder of this paper, the task of inserting a T-shaped object into a C-shaped slot is used to describe the compliant motion control algorithm and conduct a hardware experiment. The concavities of the T shape is used to insert it into a C shape whose slot width is smaller than the width of the T. It is a 3 degree of freedom problem, 2 for translation and 1 for rotation. This example has been inspired by an experiment that make a blindfold human insert a T into a C -shaped slot (McCarragher, 1994). A simple path for T insertion in our work has been obtained from the experimental result from a blindfold human.

When a blindfold man inserts T into C with a

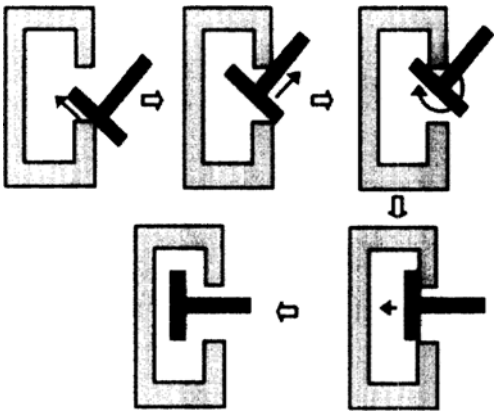

Fig. 1 Insertion sequence for T-shaped object.

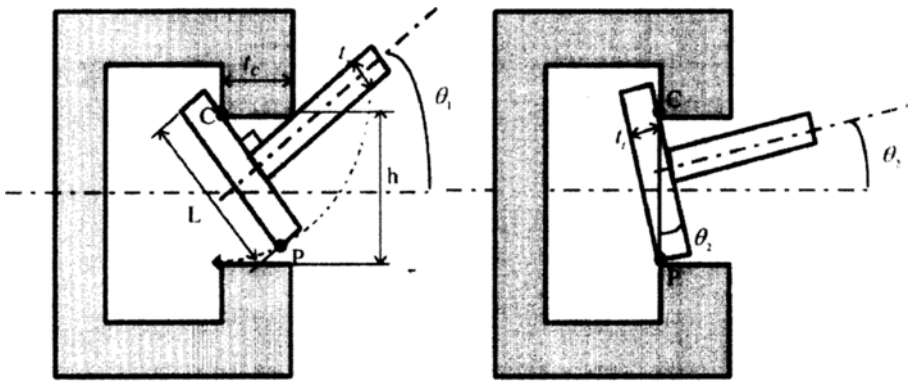

(a) Configuration of T before rotation (b) Configuration of T with two contacts

Fig. 2 Insertion conditions when rotating about C.

small clearance, he usually intends to insert it using contacts since a inserting path allowing contacts is simple to be generated and does not require fine position control. Figure 1 shows a simplified insertion path observed from human T-insertion. The dimensions of T and C-slot are determined so that at least one compliant motion has to be used to accomplish the insertion. As shown in Fig. 2(a), the geometric relation between L, the length of T, and h, the length of the entrance of C, has been derived. Assuming a fixed approach angle θ, the maximum length of $\overline{CP}$ is

$$\overline{CP}_{max}=\sqrt{\left(c_c \sin\theta_1+\frac{1}{2}t_s+\frac{L}{2}\right)^2+t_t^2}. \quad (1)$$

When T has been rotated from to about contact point C, from the relation that $\overline{CP}_{max}=h$ in Fig. 2 (b), the maximum length of L is described as

$$L_{max}=2\left(\sqrt{(h^2-t_t^2)}-t_c \sin\theta_1-\frac{1}{2}t_s\right). \quad (2)$$

Fig. 3 shows a kinematic simulation in IGRIP (Interactive Graphic Robot Instruction Program) to verify the geometrical result of the task analysis for T-insertion.

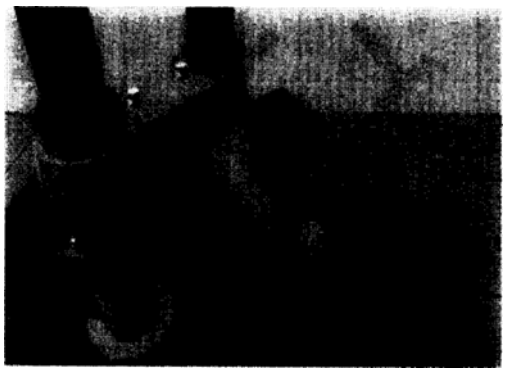

Fig. 3 Kinematic simulation of T-insertion.

3. Compliant Motion Controller Design

The compliant controller performs three processes: contact position sensing, compliance frame updating and compliant control that incorporates the above two processes. We first describe the advantages of updating the compliance frame during motion execution.

3.1 Compliance frame updating

Compliant motion control schemes including Cartesian stiffness control (Salisbury, 1980; Newman and Doring, 1991) used in this paper maintain a desired stiffness at the compliance frame, which is typically set to the point of the object in robot's hand that makes contact with other object in the work space. During an insertion task, if the contact point moves by a large amount on the surface of the object being inserted, it is necessary to move the compliance frame so it coincides with the contact point. It is especially true for tasks involving large or complex objects. When the contact point has been translated or rotated to

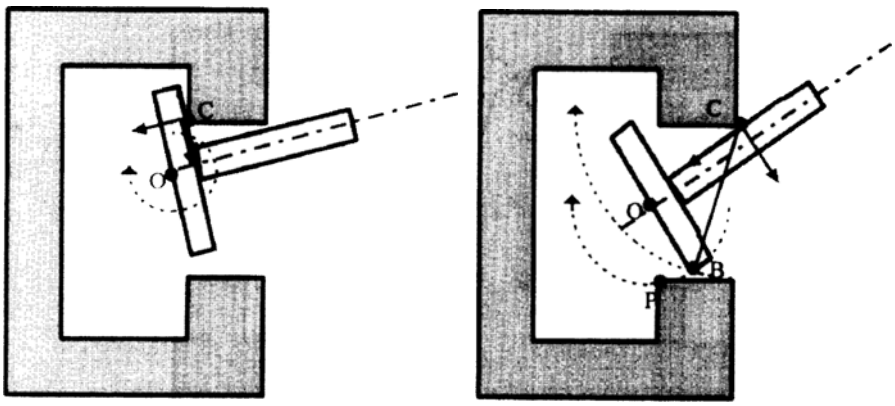

(a) Large contact force at C (b) Collision near P

Fig. 4 Problems when rotating about non-contact point O.

another one on the object surface, the stiffness gain should be adjusted to the coordinates of the compliance frame corresponding to the new contact location. If the compliance frame is set to an arbitrary fixed point on the object surface regardless of the contact point, some problems may occur depending on the location of the contact point and the geometry of the object as follows. As shown in Fig. 4(a), if T rotates about a fixed end-point O and not about the contact point C, it may exert a large undesirable force at C resulting in a positional error at O. Another reason to rotate an object about the contact point is shown in Fig. 4(b). The success of an insertion process depends on whether the T shape can pass through the smallest portion of the C slot. A good strategy is to move the T all the way to one side of the slot, and rotate it against the contact point. In Fig. 4 (b) rotation about C has a smaller chance of hitting the lower part of the C slot than rotating about O.

3.2 Contact position sensing

To locate a compliance frame to the current contact point during insertion, the location of the contact point should be determined with respect to hand frame or F/T sensor frame. Though the locations of the contact points might be estimated geometrically in the path planning stage, they may not be accurate due to various control errors during insertion. There are on-line contact-point localization algorithm developed based on F/T sensors or tactile sensors. In the case of a task where the contact point is on the object in the robots' hand rather than on the robot hand, a F/T sensor attached to the hand frame has to be used rather than tactile sensor array. Zhou, Shi and Li (1996) presented a method to localize a contact point of a tool whose shape is cylindrical or spherical. Generally, the location of the contact point can not be determined uniquely from the sensed contact force and moment, F alone. The geometric constraint $\varphi(r)=0$ describing the surface of the tool has to be imposed to get a finite number of solutions. Let Γ be the relation between the contact position vector r and the contact force F,

$$r=\Gamma(F,\ \varphi). \tag{3}$$

Since the T shape consists of two rectangular blocks, the contact localization algorithm (Zhou, Shi, and Li, 1996) is extended to rectangular

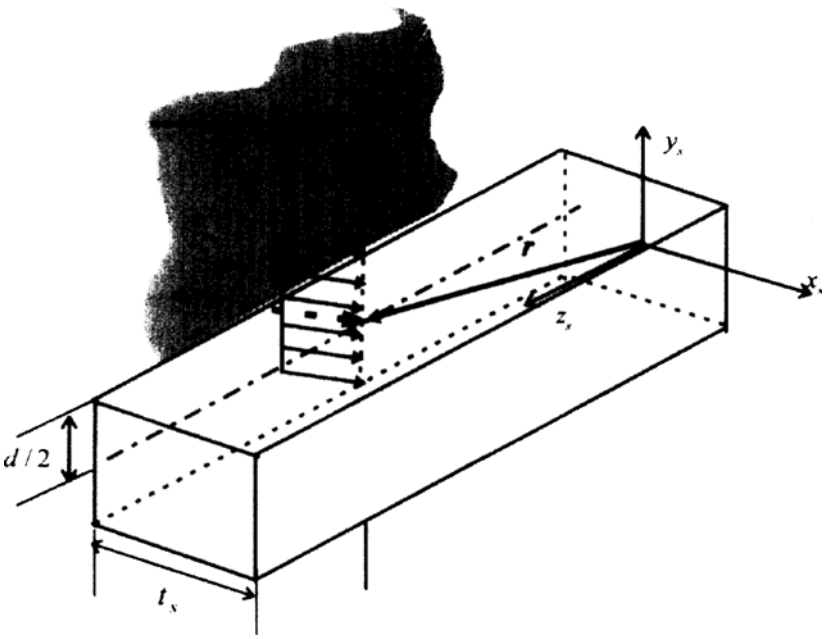

Fig. 5 Estimation of equivalent contact position r by resultant contact force.

shapes. Furthermore, since the T moves in the (X, Y, α) space, it always makes a plane-edge contact where the edge is vertical. An equivalent contact point is defined as the average of all contact points, which is the mid-point of the plane-edge contact shown in Fig. 5. In each of the 5 stages of the insertion operation in Fig. 1, only one contact exists except for the third stage. Since the thickness of the C-
shape is small, the two point contact can also be considered as a single point contact. It is also obvious at each stage which of the two rectangular blocks of the T shape makes a contact with C shape.

As mentioned above, the location of the equivalent contact point $r=(r_x, r_y, r_z)$ can be determined as follows using the sensed forces $f_s=(f_x, f_y, f_z)$, the sensed torques $\tau_s=(\tau_x, \tau_y, \tau_z)$ from F/T sensor and the geometric constraint of the rectangular cross section of T. The relation between the resultant force F acting on the equivalent contact point and the measured F/T sensor data (f, τ) is

$$f_s=F \tag{4}$$

and

$$\tau_s=r\times f_s. \tag{5}$$

Equation (5) can be rewritten as a matrix equation using a skew symmetric matrix $\hat{f}_s$,

$$\tau_s=\hat{f}_s r \tag{6}$$

$$\text{where } \hat{f}_s=\begin{bmatrix} 0 & -f_z & f_y \\ f_z & 0 & -f_x \\ -f_y & f_x & 0 \end{bmatrix}.$$

A unique solution cannot be determined from (6) because the rank$(\hat{f}_s)$ is always 2.Thus considering the geometry of the rectangular cross-section of T and the planar motion for T insertion, r can be determined as

$$r_s=\begin{cases} -t_s/2 \text{ if } f_x>0 \\ t_s/2 \text{ if } f_x<0 \end{cases} \tag{7}$$

$$r_y=0 \tag{8}$$

$$r_z=\frac{\tau_y+f_z r_x}{f_x} \tag{9}$$

The sign of r_x can be found from the sign of f_x as in (7). The computed distance r_z from measured forces and torques is shown in Fig. 6.The cut-off

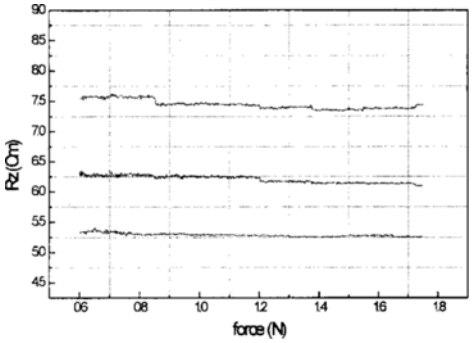

Fig. 6 The results of contact localization.

frequency of low-pass filter in F/T sensor was set to 125 Hz. The threshold force that produces a meaningful distance value is about 0.6 N. After the experiments for various distances, 52.5, 62.5 and 72.5 mm, the maximum error is around 2.5 mm-it is due to flexibility in the object, holder and F/T sensor. The computed contact position vector r is then used in real-time to modify both the forward kinematic function and Jacobian which use r as the last link dimension during insertion.

3.3 Controller design

The compliant motion controller implemented for T insertion is based on the Cartesian stiffness control. It can also be used as a high stiffness PD-type position controller for free space motion since they are the same in structure except the stiffness gain. The control law for free space motion is

$$\tau={}^tJ^T[{}^tK_d({}^tX_d-{}^tX)-{}^tB_d{}^t\dot{X}] \tag{10}$$

where, ${}^tX_d$, ${}^tX$, ${}^t\dot{X}$, and ${}^tJ^T$ are the desired trajectory, actual feedback trajectory, actual feedback velocity and transposed Jacobian with respect to the tool frame, respectively. ${}^tK_d$ and ${}^tB_d$ the high stiffness proportional gain and the derivative gain with respect to the tool frame, respectively.

In compliant motion, the desired stiffness Kd and the desired damping Bd is designed with respect to the compliance frame at the contact point. The control law including force feedback is

$$\delta\tau={}^cJ^T[{}^cK_d({}^c_d-{}^cX)-{}^cB_d{}^c\dot{X}-{}^cF] \tag{11}$$

where, ${}^cX_d$, ${}^cX$, ${}^cJ^T$, and sensed force ${}^cF$ are expressed with respect to the compliance frame at the contact point. The force feedback loop using ${}^cF$ has been added to compensate for the uncertainty in stiffness caused by a rough surface of the environment.

In designing the desired stiffness ${}^ck_x$, ${}^ck_y$, ${}^ck_\alpha$ of the diagonal matrix, ${}^cK_d$, a low stiffness is set to the direction having a motion constraint while high stiffness is set to the direction of the commanded motion. The high stiffness can, of course, be set to that of position controller ${}^tK_d$ mentioned above. On the other hand, the low stiffness in the constrained direction can be set to the ratio of tolerable contact force F_{tol} to tolerable position error X_{tol} (Hogan, 1985). For the situation shown in Fig. 7, high stiffness gains are set for X and α direction while a low stiffness is set for Y direction of the compliance frame. Thus the desired stiffness matrix can be set to

$$ {}^cK_d=\begin{bmatrix} k_x & 0 & 0 \\ 0 & F_{tol}/y_{tol} & 0 \\ 0 & 0 & k_a \end{bmatrix} \tag{12}$$

To make the closed loop dynamics have a critically damped response, assuming the inertia matrix be identity for a quasi-static motion, the desired damping matrix B_d can be set to

$$ {}^cB_d=2\sqrt{{}^cK_d}. \tag{13}$$

To maintain the compliance frame at the contact point in the compliant motion control during insertion, the last link parameter in the forward kinematics $\Lambda(q, r)$ and Jacobian ${}^cJ(q, r)$ are updated using r computed from (7), (8) and (9). The block diagram of the compliant motion control for T insertion is shown in Fig. 8.

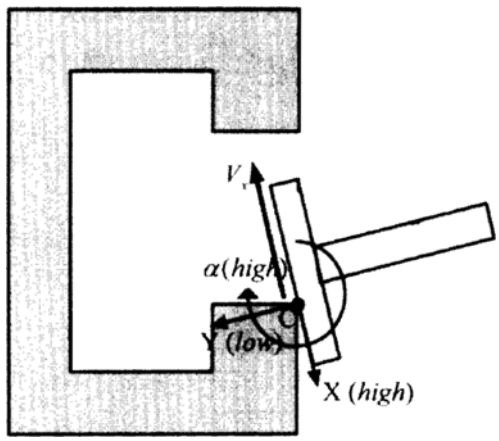

Fig. 7 Stiffness design using compliance frame.

4. Implementation and Experiment

A VME-bus based robot control system, as shown in Fig. 9, which runs in real time OS (VxWorks) has been developed to implement the T insertion. To share the computational loads, a KVME040 CPU board performs the computation for trajectory planning and contact-point localization using JR3 F/T sensor feedback, while a TMS320C30 DSP board handles the computation for stiffness control. The interface between CPU board and DSP board is done by a dual-port RAM to minimize the communication time. This

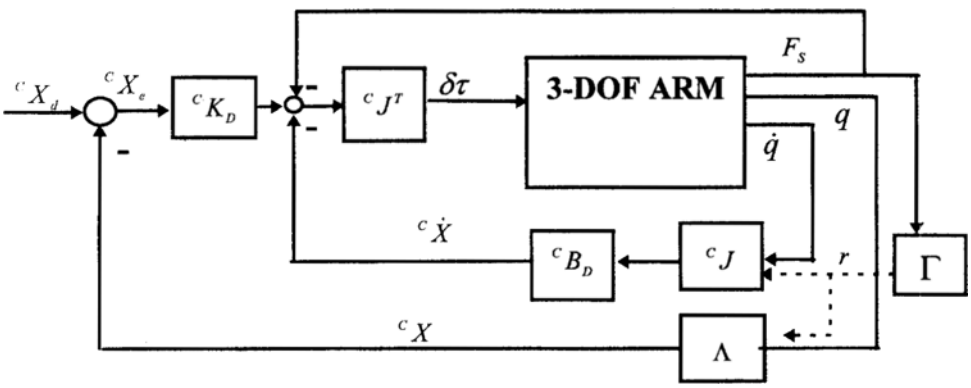

Fig. 8 Block diagram of compliant motion control system.

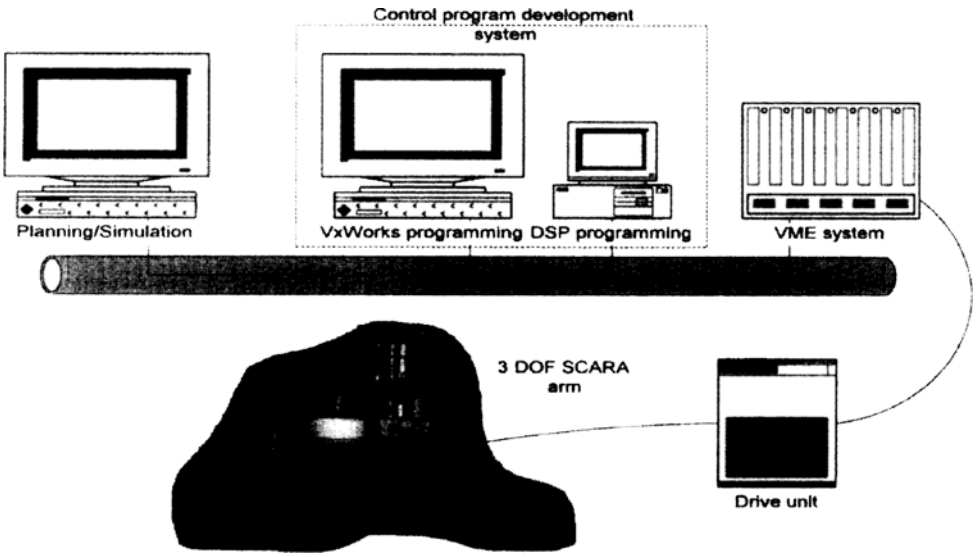

Fig. 9 VME-based real-time control system.

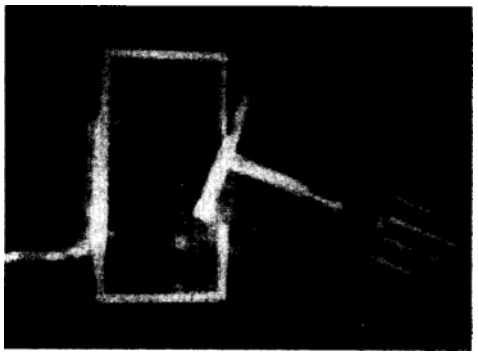

Fig. 10 T Insertion experiment.

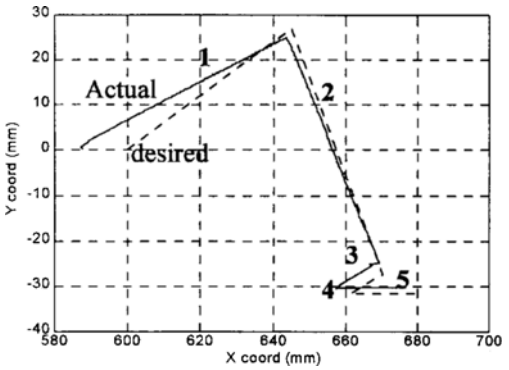

Fig. 11 Command and actual trajectory of the end-point of T insertion.

hardware architecture has achieved the trajectory update rate of 200 Hz and feedback servo rate of 1000 Hz.

The robot used in the T insertion is Goldstar GHR350-II SCARA robot which is similar to an Adept robot. To make the robot move in direction in task coordinates for T insertion, it

has been reconstructed to a 3-DOF by freezing the third prismatic joint. The T-insertion robot control system and T-insertion are shown in Fig. 10.

In the T insertion experiment, a nominal insertion path has been planned to have the contact between T and C occurs at only one point to simplify the algorithm for contact point localization and to avoid jamming. The nominal insertion path ${}^{o}X_d$ is expressed by the trajectory of the point O defined in Fig. 4(a) with respect to robot's base frame. Using the information of the contact location, ${}^{o}X_d$ is modified to ${}^{c}X_d$ on-line. The total insertion time was set to 50 sec. The actual Cartesian trajectories from T insertion is shown in Fig. 11.At the 4th stage in Fig. 11, the T rotates to enter the slot. There are some offsets between the desired path and actual path to ensure contacts in insertion. The measured forces Fx, Fy with respect to the compliance frame is shown in Fig. 12.The forces are controlled to a proper bound to maintain the force tolerance (5 kgf) by the stiffness controller with force feedback.

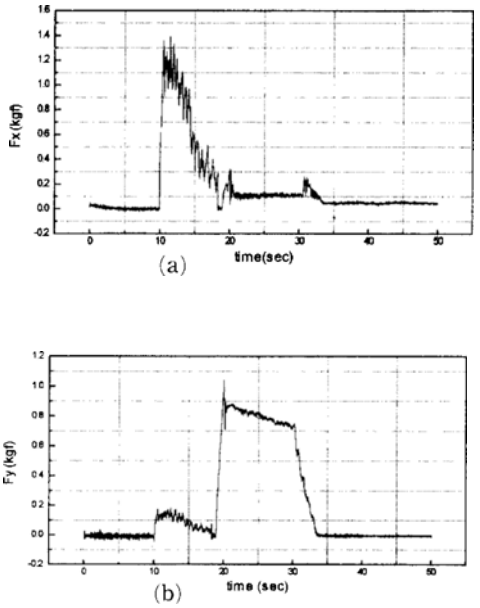

Fig. 12 Measured forces Fx(a), Fy (b) in T insertion.

5. Conclusions

To insert a complex shape using compliance, this paper presents a compliant control algorithm which is capable of rotating the object about a moving compliance frame at a contact point. A contact localization method for an object having a rectangular cross-section has been described. Furthermore, a moving compliance frame method using the location of the contact point in stiffness control loop for compliant insertion has been presented. To illustrate the performance of our algorithm, the task inserting a T into a C shape has been performed in a VME-bus based real time control system.

Two future research problems can be proposed on the insertion of complex shapes. Firstly, development of a geometric algorithm for determining the feasibility of inserting a general concave 3-dimensioanl object using contact is required. Secondly, a method for localization of contact point needs to be developed for a general object whose geometric surface constraints are semi-algebraic, i. e., intersections and unions of algebraic surfaces.

References

Asada, H. and Hirai, S., 1989, "Towards a symbolic-level force feedback: recognition of assembly process states," *Proc. of 5th Int. Symp. on Robotics Research, Tokyo,* Japan, pp. 290 ~295

Astuti, P. and McCarragher, B. J., 1996, "Discrete event controller synthesis for the convergence of an assembly process," *Proc. of the IEEE Int. Conf. on Robotics and Automation,* pp. 1153~1158

Brost, R. C. and Christiansen, A. D., 1994, "Probabilistic analysis of manipulation tasks: A computational framework," *Technical Report SAND92-2033,* Sandia National Laboratories, Albuquerque, NM, January

Canny, J. F., 1989, "On computability of the fine motion plan," *Proc. of the IEEE Int. Conf. On Robotics and Automation,* pp. 177~182

Erdmann, M., 1986, "Using backprojection for the fine motion planning with uncertainty," *Int. J. Robotics research, Res.* 5 (1), pp. 19~45

Goldenberg, A. A. and Song, P., 1996, "Analysis and design of position/force controllers Part I, II," *Workshop3 of IEEE Int. Conf. on Robotics and Automation: Force and Contact Control in Robotic Operation : Theory and Applications,* pp. 2-1~2-60.

Hogan, N., 1985, "Impedance control: an approach to manipulation: part III-applications," *ASME Journal of Dynamic Systems, Measurement and Control,* Vol. 107, pp. 17~24

Latombe, J. C., Lazanas A. and Shekhar, S., 1991, "Robot motion planning with uncertainty in control and sensing," *Artificial Intelligence,* Vol. 52, pp. 1~47,

Lee, S. and Asada, H., 1994, "Assembly of parts with irregular surface using active force sensing," *Proc. of the IEEE Int. Conf. on Robotics and Automation,* pp. 2639~2645

Lozano-Perez, T., Mason, M. T. and Taylor, R. H., 1984, "Automatic synthesis of fine motion strategies for robotics," *Int. J. Robotics Research, Res.* 3 (1), pp. 3~24

McCarragher, B. J., 1994, "Force Sensing from

Human Demonstration: Stiffness, Impedance, and Kinesthetic Sensibility," *Proc. of the IEEE/RSJ Int. Conf. on Intelligent Robots and Systems,* pp. 1226~ pp. 1233

McCarragher, B. J., 1996, "The unsupervised learning of assembly using discrete event control,", *Proc. of the IEEE Int. Conf. on Robotics and Automation,* pp. 1172~1177

Newman, W. S. and Doring, M. E., 1991, "Augmented impedance control: an approach to compliant control of kinematically redundant manipulators," *Proc. of the IEEE Int. Conf. on Robotics and Automation,* pp. 30~35

Paul, R. and Shimano, B., 1976, "Compliance and control,", *Proc. the Joint Automatic Control Conference,* ASME, pp. 694~699.

Salisbury, J. K., 1980, "Active stiffness control of a manipulator in Cartesian coordinates," *Proc. of the 19th IEEE Conf. on Decision and Control,* pp. 95~100

Strip, D. R., 1988, "Insertions using geometric analysis and hybrid force-position control: Method and analysis," *Proc. of the IEEE Int. Conf. on Robotics and Automation,* pp. 1744~1751

Tsujimura, T. and Yabuta, T., 1989, "Object detection by tactile sensing method employing force/torque information," *IEEE Trans. on Robotics and Automation,* Vol. 5, No. 4, pp. 444~450

Vukobratovic, M. and Stokic, D., 1982, *Scientific Fundamental of Robotics 2 : Control of Manipulation Robots, Theory and Application,* Springer-Verlag. Berlin, pp. 300~320

Whitney, D. E., 1977, "Force feedback control of manipulator fine motions," *ASME J. of Dynamic Systems, Measurement and Control,* Vol. 99, No. 2, pp. 91~97

Yong, B., 1997, "Contour-following of a force-controlled industrial robot using preview control," *KSME International Journal,* Vol. 11, No. 2, pp115~122

Zhou, X., Shi, Q. and Li, Z., 1996, "Contact localization using force/torque measurements," *Proc. of the IEEE Int. Conf. on Robotics and Automation,* pp. 1339~1344